

PROGRESS TOWARDS HIGH-QUALITY, HIGH-REPETITION-RATE PLASMA ACCELERATION AT FLASHForward

J. C. Wood^{*,1}, L. Boulton¹, J. Beinortaitė^{1,2}, J. Björklund Svensson¹, G. Boyle¹, J. Cowley³, A. Ferran Pousa¹, B. Foster^{1,2}, M. J. Garland¹, P. González-Caminal¹, M. Huck¹, H. Jones¹, A. Kanekar¹, C. A. Lindstrøm^{1,4}, G. Loisch¹, T. Long¹, S. M. Mewes¹, J. Osterhoff¹, F. Peña¹, S. Schröder¹, M. Thévenet¹, S. Wesch¹, M. Wing^{1,2} and R. D'Arcy^{1,3}

¹Deutsches Elektronen-Synchrotron DESY, Hamburg, Germany

²University College London, United Kingdom

³University of Oxford, United Kingdom

⁴University of Oslo, Norway

Abstract

Plasma-wakefield acceleration represents an exciting route towards reducing the footprint of future high-energy electron accelerators by accelerating bunches in fields exceeding 1 GV/m. One such technique employs a double-bunch structure where the trailing bunch is accelerated in the field of a high-amplitude plasma-density wake driven by the leading bunch. A future particle collider or photon science facility incorporating plasma accelerators will be required to accelerate up to millions of bunches per second with high energy efficiency while preserving the brightness of the accelerating bunch. This contribution presents the latest progress towards these goals at FLASHForward (DESY).

INTRODUCTION

Electron-bunch-driven plasma wakefield accelerators (PWFAs) [1, 2] have the potential to greatly extend the energy reach of existing and future electron accelerators in a compact footprint by boosting the energy of bunches in fields $> 1 \text{ GV m}^{-1}$. A short, relativistic electron bunch of density n_b travelling through an underdense plasma of density $n_e \ll n_b$ will expel all nearby plasma electrons, driving a fully-cavitated plasma wake that travels at close to the speed of light [3, 4]. The heavier plasma ions barely move over short timescales, providing linear focussing fields that can preserve bunch quality [5], and a strong longitudinal field providing rapid, phase-locked acceleration for a trailing bunch. By shaping the trailing bunch, the wakefield can be loaded to preserve the energy spread of the entire trailing bunch, while simultaneously transferring energy from the driver to the trailing bunch with high efficiency [6, 7].

FLASHForward is a plasma acceleration experiment using high-quality electron bunches from the linac of the FLASH FEL [8], with the goal of developing plasma technologies to match the beam-quality-preserving and high-repetition rate acceleration of radiofrequency accelerators. Notable results include the preservation of transverse emittance during acceleration [5], the preservation of per-mille energy spread [9], and the demonstration that plasma accelerators can recover rapidly enough to support $O(10 \text{ MHz})$ interbunch repetition rates [10].

Ref. [9] also showed that the instantaneous transfer efficiency, meaning the energy gained by the trailing bunch divided by the energy lost by the driver, was as high as $(42 \pm 4) \%$. Further experimental studies showed that $(59 \pm 3) \%$ of the driver bunch energy can be deposited into the plasma before part of the driver bunch was completely decelerated [11]. These results suggest that a plasma stage with an overall efficiency (trailing bunch energy gain divided by initial driver energy) of tens of percent could be within reach. Recent results from FLASHForward are presented in this paper, working towards this goal. In a useful PWA, a large trailing bunch charge must be coupled into the wakefield and accelerated with low energy spread. Wakefield acceleration can be affected by many input parameters, therefore, Bayesian optimisation routines have been employed to control the acceleration process. This paper reports on optimisation results from a 50 mm plasma cell, followed by a demonstration of acceleration by more than 200 MeV in a 195 mm plasma. To push the overall efficiency higher in our setup, a 500 mm discharge plasma source was developed and its characterisation is described.

EXPERIMENTAL SETUP

The FLASH linac and FLASHForward are described in Refs. [8, 12]. After a recent upgrade, FLASH now delivers electron bunches with energies up to 1.35 GeV [13]. To maintain flexibility in the RF settings for longitudinal bunch shaping, FLASHForward typically operates with a bunch energy of 1.2 GeV. Single bunches with charges up to $\sim 850 \text{ pC}$ are accelerated and compressed to peak currents of $\sim 1 \text{ kA}$. Third harmonic cavities are used to linearise the longitudinal phase space, and a laser heater has recently been commissioned to suppress microbunching [14]. The drive and trailing bunches are created using a variable notch collimator in the final dispersive section [15]. In this paper, post-optimisation, the driver and trailing bunches had incoming charges of 230 pC and 50 pC, with root-mean-square (RMS) durations of 110 fs and 40 fs, respectively. They had typical normalised emittances of 3-4 mm mrad and $\sim 1 \text{ mm mrad}$ respectively. They were focussed by a set of quadrupoles to $O(10 \text{ mm})$ β -functions at the start of a discharge-ionised plasma contained within a sapphire capillary without endcaps. In the results reported below, the

* jonathan.wood@desy.de

optimum $n_e \sim 8 \times 10^{15} \text{ cm}^{-3}$. The primary bunch diagnostics are one broadband and one high-resolution imaging spectrometer for energy and emittance measurements, and an X-band transverse deflection structure coupled with a dipole for longitudinal phase space characterisation [16].

AUTOMATED OPTIMISATION OF PWFA

Bayesian optimisation has gained popularity as an efficient optimisation technique in radiofrequency and plasma accelerator physics [17–21] because the output, which can be contaminated by noise, has complex dependencies on a large number of input parameters. Figure 1 shows the Bayesian optimisation, using the Optimas library [22], of the acceleration of trailing bunches through a 50-mm long plasma cell, using a Gaussian process surrogate model with expected improvement as the acquisition function. The objective function to be maximised was defined as $G = \Delta E^2 Q'_{\text{max}}$, where ΔE is the mean energy gain of the trailing bunch and $Q'_{\text{max}} = (dQ/dE)_{\text{max}}$ is its maximum spectral density, both measured using the broadband electron spectrometer. To account for random noise, G was averaged over 20 data points at each iteration. Four variables were exposed to the optimiser: the chirp h applied to the bunch in an RF module controlling bunch compression, the position of the wedge collimator x_{wedge} that divided the initial bunch in to the driver-trailing bunch pair, the current of a quadrupole I_Q in a chicane that controlled the 1st-order horizontal dispersion, and the timing of the discharge t_d that varied n_e . The evolution of these parameters is shown in Fig. 1 (b). Beginning from a manually-found point where the value of G was low—the trailing bunch started with $Q'_{\text{max}} = 6 \text{ pC MeV}^{-1}$ and $\Delta E = 20 \text{ MeV}$ —the optimiser first performed some initial exploratory steps (iterations 0–10) where the input parameters were changed simultaneously by relatively large amounts. Following this, the optimiser maximised G after 28 iterations. The resulting working point had an energy gain of $(103 \pm 1) \text{ MeV}$, corresponding to an average accelerating gradient of 2.1 GV m^{-1} . This came at the expense of spectral density $Q'_{\text{max}} = (2.4 \pm 0.2) \text{ pC MeV}^{-1}$ largely due to only $(34 \pm 2) \text{ pC}$ emerging from the plasma, a natural result of the heavy weighting of ΔE in G . These results provide an early example of the automated optimisation of plasma acceleration at FLASHForward, with the eventual goal that this can become an efficient, semi-automated alternative to the time-consuming manual setup of PWFA stages in the future.

ACCELERATION TO HIGHER ENERGIES

Plasma acceleration at FLASHForward is limited to maximum acceleration gradients $\propto \sqrt{n_e}$ of $1\text{--}2 \text{ GV m}^{-1}$. The restriction on the plasma density is that both the driver and the trailing bunch, which should carry considerable charge, must fit into the first wakefield period. Stronger bunch compression can, therefore, lead to higher acceleration gradients, although this risks degradation of the bunches from coherent synchrotron radiation effects in the bunch compressors. The

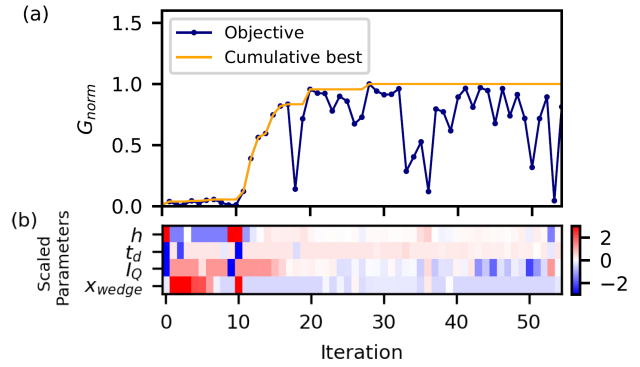


Figure 1: Optimisation plots. (a) The objective function G evolves with iteration number (blue). The orange line shows the cumulative best G that was achieved. Changes in the four input parameters during the optimisation are shown in (b). G is normalised to its maximum value whilst the input parameters were scaled to have a mean value of zero and a standard deviation of 1 over the whole optimisation.

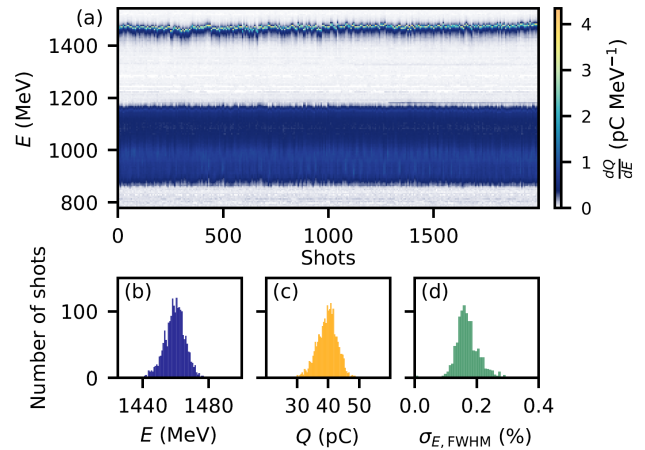


Figure 2: Acceleration in a 195 mm plasma cell. (a) Energy spectra of 2000 consecutive acceleration events, with an imaging energy of 1450 MeV. Shown below are histograms of the trailing bunch mean electron energy (b), charge (c) and FWHM percentage energy spread (d).

bunch length and n_e used at FLASHForward represents a balance between desiring high bunch quality and rapid plasma acceleration. In order to produce high energy gains with simultaneous high overall energy efficiency, it is necessary to use a long plasma cell.

The first step towards this was taken by attempting to accelerate many tens of pC at 1 GV m^{-1} in a 195 mm-long plasma cell. Figure 2 (a) displays driver and trailing-bunch spectra from this cell, where the scraper position and width were manually altered from the optimised working point from the 50 mm cell. Figure 2 (b) displays a histogram of the measured trailing bunch energy. Trailing bunch acceleration from 1208 MeV to $(1460 \pm 6) \text{ MeV}$ was observed—an energy gain of $(252 \pm 6) \text{ MeV}$ at 1.3 GV m^{-1} . The energy uncertainty is the standard deviation, which is at the level of 2.6 %. Similar histograms are shown for the charge and full width at half maximum (FWHM) percentage energy spread

of the trailing bunches in Fig. 2 (c) and (d), with mean values of $Q = (40 \pm 3)$ pC and $\sigma_{E,FWHM} = (0.17 \pm 0.04)$ %, respectively, the latter being measured on a narrowband spectrometer with higher spectral resolution. The average total energy gained by the trailing bunch was $\Delta W = Q\Delta E = (10 \pm 1)$ mJ, which for the incoming driver with a charge of 230 pC and mean electron energy of 1200 MeV corresponds to an overall energy transfer efficiency of (3.6 ± 0.3) %.

A PLASMA TARGET FOR HIGH-EFFICIENCY ACCELERATION

Using the same input bunch parameters and a half-metre plasma with $n_e \sim 8 \times 10^{15} \text{ cm}^{-3}$ there is the prospect of achieving energy gains of at least 0.5 GeV. With this motivation, a discharge plasma cell was designed around a 500 mm sapphire tube with a 1.7 mm inner diameter and 4.3 mm outer diameter, and it was characterised in DESY's ADVANCE Lab [23]. An image of a plasma formed in this capillary is shown in Fig. 3 (a). A mixture of 97 % Ar, 3 % H_2 gas was fed into the cell from a buffer held at 9.25 mbar via a mass flow controller at a rate of $0.14 \text{ mbar l s}^{-1}$. To aid with reproducible plasma generation, a 'glow discharge' was used. This is a low-ionisation-state plasma maintained by a constant applied voltage of 3.2 kV. To produce the desired plasma densities for acceleration a 20 kV, microsecond duration voltage pulse was applied across the existing low-density plasma. An example current trace, which had a typical amplitude of 290 A, is shown in Fig. 3(b).

The plasma density was measured via the pressure broadening of the H_α line measured via emission spectroscopy, based on calculations from Refs. [24, 25] and following the experimental method detailed in Ref. [26]. The emitted spectra were analysed using an imaging spectrometer with a 900 lp mm^{-1} grating with a $50 \mu\text{m}$ slit imaged on to an intensified CCD camera with a 100 ns integration time. A slice of the plasma close to the longitudinal centre of the cell was imaged on to the slit with magnification of 1 radially and 1/6 longitudinally. The minimum density that can be resolved in this setup is approx. $5 \times 10^{14} \text{ cm}^{-3}$. The temporal evolution of the density was measured by scanning the ICCD camera trigger timing with respect to the discharge trigger, and is shown in Fig. 3 (b). This plot also demonstrates the longevity of the cell. Between density evolution scans, the discharge repetition rate was set to 5 Hz and run for 1 h. A total of 6.6×10^4 high-voltage discharges were applied to the cell without damaging it. n_e did not drift but rather jittered with <3 % rms amplitude at the hourly measurements.

The working point detailed in Fig. 2 is achievable in the 500 mm capillary at a discharge delay of approx. $4.6 \mu\text{s}$. The rms jitter of the discharge timing was calculated from 1000 consecutive current traces to be 12 ns. At a delay of $4.6 \mu\text{s}$, $dn_e/dt = -0.3 \times 10^{16} \text{ cm}^{-3} \mu\text{s}^{-1}$, meaning that the density jitter due to the discharge timing jitter is approx. $3.6 \times 10^{13} \text{ cm}^{-3}$, or 0.4 %. In separate measurements, at a slightly different buffer pressure of 8.37 mbar and the ICCD timing adjusted to measure a density of

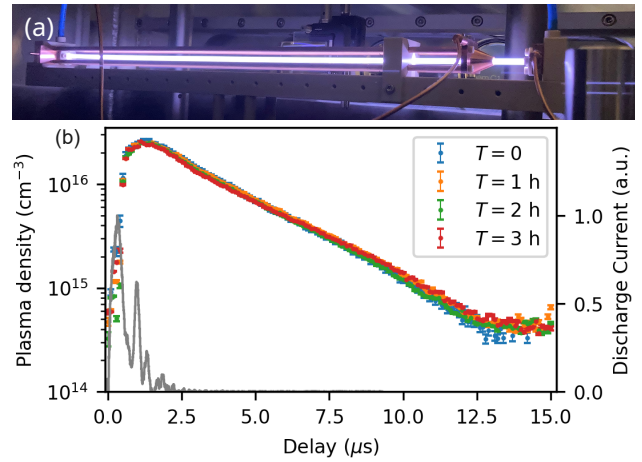


Figure 3: Generation and characterisation of a 500 mm long discharge capillary. (a) Image of the plasma cell. (b) Plasma density versus delay from the plasma ignition, measured after multiple hours of continuous operation. Each point averages over 20 events. The grey curve is an example input discharge current trace.

$1.04 \times 10^{16} \text{ cm}^{-3}$, the rms deviation of the measured plasma density over 1000 consecutive measurements was 1.8 %, or $2 \times 10^{14} \text{ cm}^{-3}$. Since this is significantly smaller than the resolution limit of $5 \times 10^{14} \text{ cm}^{-3}$, this measurement may have been instrument limited.

The 500 mm cell presented here is capable of producing the required electron density with percent-level shot-to-shot variations, and can do so for $\mathcal{O}(10^5)$ events without a significant change in performance. It is, therefore, a highly promising solution for near-future experimentation, where we realistically aim to increase the trailing bunch energy from 1.2 to 1.7 GeV with high overall efficiency.

CONCLUSION

FLASHForward continues to advance plasma accelerator technologies towards the high quality, efficiency and repeatability required for many applications. To enhance this progress in the future, Bayesian optimisation techniques have been incorporated into the accelerator control software. Initial tests confirm that an optimum can be rapidly found by varying four important parameters simultaneously. To improve on the energy gain of the trailing electron bunches, and to boost the overall energy efficiency of the plasma accelerator at FLASHForward, acceleration with per-mille-level energy spread acceleration from 1208 to 1460 MeV in a 195 mm plasma was demonstrated over 2000 consecutive shots. A 500 mm plasma cell has been constructed within specifications for experimentation in the near future towards higher energy gains and efficiencies.

ACKNOWLEDGEMENTS

The authors thank M. Dinter, S. Karstensen, S. Kotler, K. Ludwig, F. Marutzky, A. Rahali, V. Rybnikov and A. Schleiermacher. The authors acknowledge funding from Helmholtz ARD.

REFERENCES

- [1] T. Tajima and J. M. Dawson, "Laser electron accelerator", *Phys. Rev. Lett.*, vol. 43, no. 4, pp. 267–270, 1979. doi:10.1103/PhysRevLett.43.267
- [2] P. Chen, J. M. Dawson, R. W. Huff, and T. Katsouleas, "Acceleration of electrons by the interaction of a bunched electron beam with a plasma", *Phys. Rev. Lett.*, vol. 54, no. 7, pp. 693–696, 1985. doi:10.1103/PhysRevLett.54.693
- [3] A. Pukhov and J. Meyer-ter-Vehn, "Laser wake field acceleration: the highly non-linear broken-wave regime", *Appl. Phys. B Lasers Opt.*, vol. 74, pp. 355–361, 2002. doi:10.1007/s003400200795
- [4] W. Lu, C. Huang, M. Zhou, W. B. Mori, and T. Katsouleas, "Nonlinear theory for relativistic plasma wakefields in the blowout regime", *Phys. Rev. Lett.*, vol. 96, no. 16, p. 165 002, 2006. doi:10.1103/PhysRevLett.96.165002
- [5] C. A. Lindstrøm *et al.*, "Emittance preservation in a plasma wakefield accelerator", *ArXiv*, 2024. doi:10.48550/arXiv.2403.17855
- [6] M. Tzoufras *et al.*, "Beam loading in the nonlinear regime of plasma-based acceleration", *Phys. Rev. Lett.*, vol. 101, no. 14, p. 145 002, 2008. doi:10.1103/PhysRevLett.101.145002
- [7] C. Lindstrøm and M. Thévenet, "Emittance preservation in advanced accelerators", *J. Instrum.*, vol. 17, no. 05, p. P05016, 2022. doi:10.1088/1748-0221/17/05/P05016
- [8] S. Schreiber and B. Faatz, "The free-electron laser flash", *High Power Laser Sci. Eng.*, vol. 3, p. e20, 2015. doi:10.1017/hpl.2015.16
- [9] C. A. Lindstrøm *et al.*, "Energy-spread preservation and high efficiency in a plasma-wakefield accelerator", *Phys. Rev. Lett.*, vol. 126, no. 1, p. 014 801, 2021. doi:10.1103/PhysRevLett.126.014801
- [10] R. D'Arcy *et al.*, "Recovery time of a plasma-wakefield accelerator", *Nature*, vol. 603, 2022. doi:10.1038/s41586-021-04348-8
- [11] F. Peña *et al.*, "Energy depletion and re-acceleration of driver electrons in a plasma-wakefield accelerator", *ArXiv*, 2023. doi:10.48550/arXiv.2305.09581
- [12] R. D'Arcy *et al.*, "Flashforward: Plasma wakefield accelerator science for high-average-power applications", *Philos. Trans. R. Soc. A*, vol. 377, no. 2151, 2019. doi:10.1098/rsta.2018.0392
- [13] M. Vogt, S. Schreiber, and J. Zemella, "Flash: Status and upgrade", in *67th ICFA Adv. Beam Dyn. Workshop Future Light Sources*, 2023. doi:10.18429/JACoW-FLS2023-M03A5
- [14] C. Gerth *et al.*, "Layout of the Laser Heater for FLASH2020+", in *Proc. IPAC'21*, Campinas, SP, Brazil, 2021, paper TUPAB111, pp. 1647–1650. doi:10.18429/JACoW-IPAC2021-TUPAB111
- [15] S. Schröder *et al.*, "Tunable and precise two-bunch generation at flashforward", *J. Phys. Conf. Ser.*, vol. 1596, no. 1, p. 012 002, 2020. doi:10.1088/1742-6596/1596/1/012002
- [16] P. González Caminal *et al.*, "Beam-based commissioning of a novel X-band transverse deflection structure with variable polarization", *Phys. Rev. Accel. Beams*, vol. 27, no. 3, p. 032 801, 2024. doi:10.1103/PhysRevAccelBeams.27.032801
- [17] J. Duris *et al.*, "Bayesian optimization of a free-electron laser", *Phys. Rev. Lett.*, vol. 124, no. 12, p. 124 801, 2020. doi:10.1103/PhysRevLett.124.124801
- [18] R. Roussel *et al.*, "Bayesian Optimization Algorithms for Accelerator Physics", *Tech. Rep.*, 2023. doi:10.48550/arXiv.2312.05667
- [19] A. Hanuka *et al.*, "Physics model-informed gaussian process for online optimization of particle accelerators", *Phys. Rev. Accel. Beams*, vol. 24, no. 7, p. 072 802, 2021. doi:10.1103/PhysRevAccelBeams.24.072802
- [20] S. Jalas *et al.*, "Bayesian optimization of a laser-plasma accelerator", *Phys. Rev. Lett.*, vol. 126, no. 10, p. 104 801, 2021. doi:10.1103/PhysRevLett.126.104801
- [21] R. J. Shalloo *et al.*, "Automation and control of laser wake-field accelerators using bayesian optimization", *Nat. Commun.*, vol. 11, no. 1, p. 6355, 2020. doi:10.1038/s41467-020-20245-6
- [22] A. Ferran Pousa *et al.*, "Bayesian optimization of laser-plasma accelerators assisted by reduced physical models", *Phys. Rev. Accel. Beams*, vol. 26, no. 8, p. 084 601, 2023. doi:10.1103/PhysRevAccelBeams.26.084601
- [23] J. Garland *et al.*, "A Discharge Plasma Source Development Platform for Accelerators: The ADVANCE Lab at DESY", in *Proc. IPAC'22*, 2022, paper WEPOPT021, pp. 1886–1888. doi:10.18429/JACoW-IPAC2022-WEPOPT021
- [24] M. A. Gigosos and V. Cardeñoso, "New plasma diagnosis tables of hydrogen stark broadening including ion dynamics", *J. Phys. B: At. Mol. Phys.*, vol. 29, no. 20, p. 4795, 1996. doi:10.1088/0953-4075/29/20/029
- [25] M. A. Gigosos, M. Á. González, and V. Cardeñoso, "Computer simulated balmer-alpha, -beta and -gamma stark line profiles for non-equilibrium plasmas diagnostics", *Spectrochim. Acta, Part B*, vol. 58, no. 8, pp. 1489–1504, 2003, 5th European Furnace Symposium and 10th International Solid Sampling Colloquium with Atomic Spectroscopy. doi:10.1016/S0584-8547(03)00097-1
- [26] J. M. Garland *et al.*, "Combining laser interferometry and plasma spectroscopy for spatially resolved high-sensitivity plasma density measurements in discharge capillaries", *Rev. Sci. Instrum.*, vol. 92, no. 1, p. 013 505, 2021. doi:10.1063/5.0021117